

Received: 2021.03.12

Accepted: 2021.06.01

Available online: 2021.06.15

Published: 2021.06.24

# An Individualized Contrast-Enhanced Liver Computed Tomography Imaging Protocol Based on Body Mass Index in 126 Patients Seen for Liver Cirrhosis

**Authors' Contribution:**

Study Design A  
Data Collection B  
Statistical Analysis C  
Data Interpretation D  
Manuscript Preparation E  
Literature Search F  
Funds Collection G

**ABCEG Jian Jiang**  
**BD Maowei Zhang**  
**BCDF Yuan Ji**  
**CD Chunfeng Li**  
**BF Xin Fang**  
**B Shuyuan Zhang**  
**CF Wei Wang**  
**EF Lijun Wang**  
**ACEF Ailian Liu**

Department of Radiology, The First Affiliated Hospital of Dalian Medical University, Dalian, Liaoning, P.R. China

**Corresponding Author:** Ailian Liu, e-mail: [cjr.liuailian@vip.163.com](mailto:cjr.liuailian@vip.163.com)

**Source of support:** This work was funded by the Education Department of Liaoning Province Foundation (No. LZ2019047)

**Background:** Computed tomography (CT) imaging using iodinated contrast medium is associated with the radiation dose to the patient, which may require reduction in individual circumstances. This study aimed to evaluate an individualized liver CT protocol based on body mass index (BMI) in 126 patients investigated for liver cirrhosis.


**Material/Methods:** From November 2017 to December 2020, in this prospective study, 126 patients with known or suspected liver cirrhosis were recruited. Patients underwent liver CT using individualized protocols based on BMI, as follows. BMI  $\leq 24.0$  kg/m<sup>2</sup>: 80 kV, 352 mg I/kg; BMI 24.1-28.0 kg/m<sup>2</sup>: 100 kV, 440 mg I/kg; BMI  $\geq 28.1$  kg/m<sup>2</sup>: 120 kV, 550 mg I/kg. Figure of merit (FOM) and size-specific dose estimates (SSDEs) were calculated and compared using the Mann-Whitney U test. Subjective image quality and timing adequacy of the late arterial phase were evaluated with Likert scales.

**Results:** The SSDE was significantly lower in the 80 kV protocol, corresponding to a dose reduction of 36% and 50% compared with the others (all  $P < 0.001$ ). In the comparison of 80-, 100-, and 120-kV protocols, no statistically significant differences were found in FOMs ( $P = 0.108-0.620$ ). Of all the examinations, 95.2% (120 of 126) were considered as appropriate timing for the late arterial phase. In addition, overall image quality, hepatocellular carcinoma conspicuity, and detection rate did not differ significantly among the 3 protocols ( $P = 0.383-0.737$ ).

**Conclusions:** This study demonstrated the feasibility of using an individualized liver CT protocol based on BMI, and showed that patients with lower BMI should receive lower doses of iodinated contrast medium and significantly reduced radiation dose.

**Keywords:** **Body Mass Index • Carcinoma, Hepatocellular • Radiation Dosage • Radiology**

**Full-text PDF:** <https://www.medscimonit.com/abstract/index/idArt/932109>

 2765

 6

 4

 29



## Background

Liver cirrhosis is a major cause of hepatocellular carcinoma (HCC) in Asian populations [1,2]. Liver Imaging Reporting and Data System (LI-RADS) guidelines propose contrast-enhanced liver computed tomography (CT) as an effective and valuable diagnostic method for liver cirrhosis and HCC [3]. Liver cirrhosis patients experience years of followup employing enhanced CT examination. The cumulative radiation exposure and exposure to the iodinated contrast medium and can lead to damaged renal function, bringing about further harm to patients with chronic medical conditions. Feng et al [4] showed that an individualized injection protocol might reduce the contrast medium dose used in enhanced liver CT. However, patients with liver cirrhosis were excluded from that study, and the individualized protocol was not combined with optimized CT scanning. Therefore, the question of how to individually optimize a combined CT scanning examination and injection protocol is crucial for liver cirrhosis populations.

Reduction of the tube voltage is the most efficient method for lowering the multi-detector row computed tomography (MDCT) radiation dose [5-7]. Some studies have reported that using a CT scanning protocol with an appropriate low tube voltage setting could significantly decrease the radiation dose in thin adults [8,9]. Furthermore, studies have shown that a low tube voltage CT protocol could reduce the dose of iodine contrast medium [10-12], making it possible to lower iodine administration in contrast-enhanced CT imaging. Simultaneously decreasing the tube voltage and contrast agent has been attempted and used for abdominal CT and CT angiography (CTA) [13,14] in a low body mass index (BMI) population. To our knowledge, use of a low tube voltage setting, together with a small amount of iodine injection according to the patient's BMI, has not been widely adopted in patients with liver cirrhosis.

The present study aimed to evaluate an individualized contrast-enhanced liver CT protocol based on BMI in 126 patients investigated for liver cirrhosis.

## Material and Methods

### Patient Population

This prospective, single-center Health Insurance Portability and Accountability Act (HIPAA)-compliant study received Institutional Review Board approval by the First Affiliated Hospital of Dalian Medical University. Informed consent was obtained from enrolled patients after information on risks related to iodinated contrast medium and radiation were explained to the patients. From November 2017 to December 2020, 132 consecutive patients ( $\geq 18$  years old) were enrolled

prospectively in the study. The inclusion criteria were: (1) patients with known or suspected liver cirrhosis who underwent liver MDCT; (2) absence of renal impairment; and (3) no contraindication for iodinated contrast medium. Six patients were excluded from this study because of inadequate CT examinations due to either equipment failure ( $n=2$ ) or inadequate injection due to contrast medium extravasation ( $n=4$ ). Body weight, height, and BMI data were obtained before CT examination. The patients were assigned to individualized scanning protocols based on BMI. The detailed patient selection, inclusion, and exclusion criteria are described in **Figure 1**.

### CT Scanning Protocols

CT scanning was conducted in a 64-MDCT scanner (either Optima CT660 or Discovery CT750 HD; GE Healthcare, Connecticut, USA). Multiphase liver CT scanning consisted of unenhanced, late arterial, portal venous, and delay phases. The iodinated contrast medium, with an iodine concentration of 300 mg I/mL (Ultravist, Bayer, Bayer Leverkusen, Germany), was injected into an antecubital vein with a power injector. According to Gauray et al [15], 120 kV is sufficient to provide diagnostic liver CT images suitable for application in overweight and obese populations. Some studies have also reported that reducing the radiation dose led to acceptable image quality when selection of the optimal tube voltage was based on the patient's BMI [16]. This is also the theoretical basis for the present study; to set the tube voltage at 120 kV for patients with  $\text{BMI} \geq 28.1 \text{ kg/m}^2$ , 100 kV for patients with  $28 > \text{BMI} > 24.1 \text{ kg/m}^2$ , and 80 kV for patients with  $\text{BMI} \leq 24 \text{ kg/m}^2$ . According to Ichikawa et al [17], the reduction of iodine load was 80% and 64% at 80 kV and 100 kV, respectively, compared with 550 mg I/kg at 120 kV. The parameters for CT scanning and contrast injection protocols for all examinations are shown in **Table 1**. According to Achille Mileto et al [18], results in liver cirrhosis patients with dysfunctional blood systems supported the benefits achievable with appropriate timing for the scanning phase by using a splenic-triggering protocol. Therefore, the late hepatic arterial phase was determined using the bolus-tracking technique, which entails automatically starting 15 s after the trigger threshold is met; the trigger threshold should be set at an increase of 50 Hounsfield units (HU). The trigger threshold was reached in a region of interest (ROI) drawn within the splenic parenchyma (mean pixel number of ROI trigger, 34.3). The portal venous and delayed images were obtained 70 and 180 s after the start of contrast medium injection (**Figure 2**).

### Radiation Dose

For all patients, the volume of CT dose index ( $\text{CTDI}_{\text{vol}}$ ), the dose-length product (DLP), and the effective dose (ED) were recorded (conversion factor of  $0.015 \text{ mSv mGy}^{-1} \text{ cm}^{-1}$ ) [19]. The

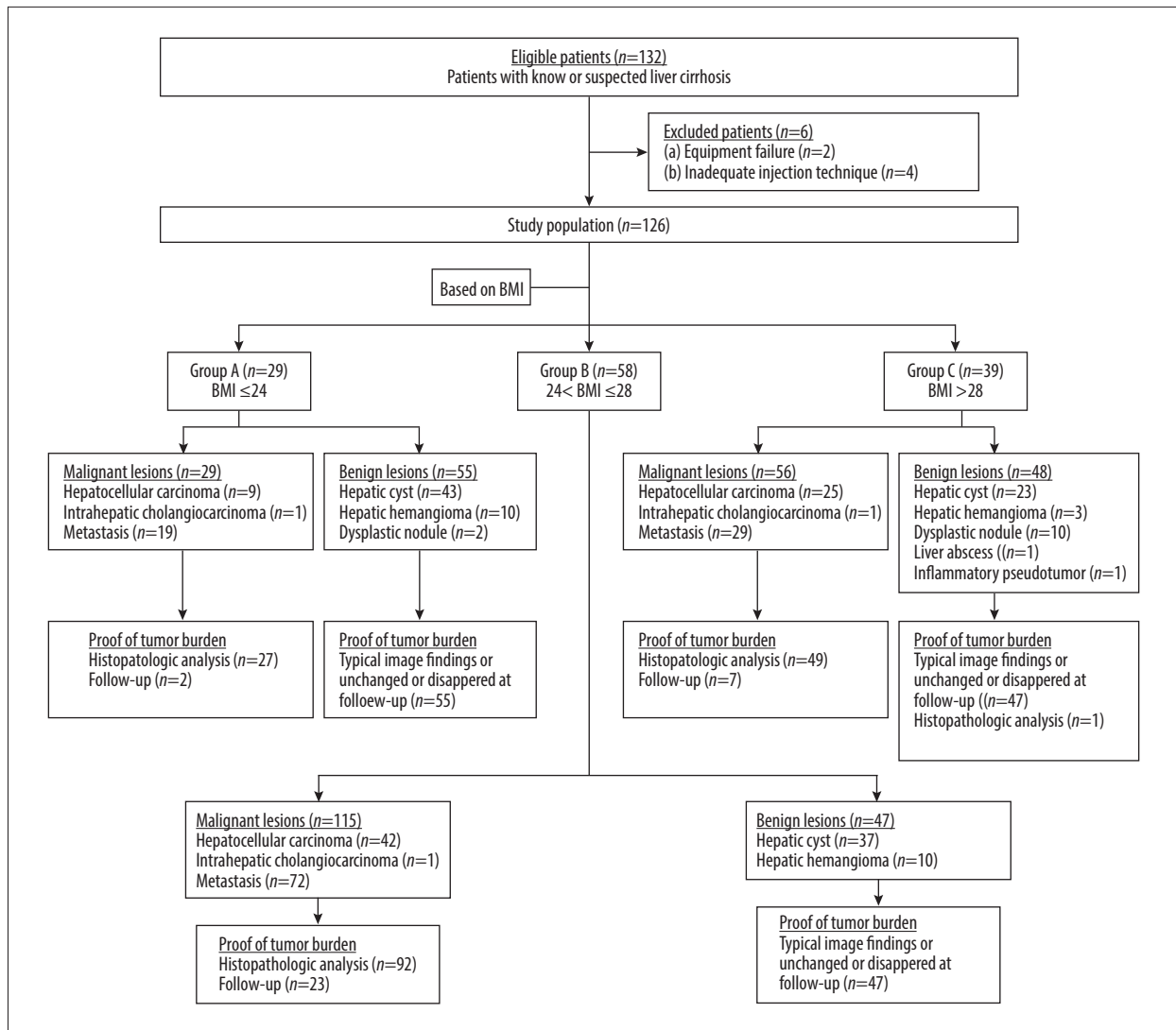


**Figure 1.** Flow diagram of the inclusion procedures performed in this study. BMI – body mass index.

size-specific dose estimate (SSDE) for the late arterial phase was calculated by using the sum of the anterior-posterior and lateral dimensions at the mid-liver level [20].

### Image Evaluation

The timing of the late arterial phase was assessed according to the LI-RADS guidelines published in 2018 [3]. The observer used a 3-point Likert scale (where 1=early, 2=appropriate, and 3=late). More specifically, the 3 Likert values indicate the following: 1, full aortic and hepatic arterial enhancement with scarce portal, hepatic parenchymal, or venous enhancement; 2, hepatic parenchymal enhancement or full hepatic arterial and aortic enhancement with mild to moderate portal enhancement and absence of antegrade enhancement of hepatic veins; 3, full aortic and hepatic arterial enhancement with moderate to high portal, hepatic parenchymal, or venous enhancement.

Both objective and subjective image quality were assessed for each patient in a blinded and randomized fashion. The objective image analysis was based on reconstructed 1-mm-thick images. For all patients, all the images were displayed in a preset soft-tissue window (level, 40 HU; width, 300 HU). The CT values for liver, pancreas parenchyma, and blood vessels were measured. Standard deviations of the attenuation of the anterior abdominal wall's subcutaneous fat were recorded to represent the objective image noise. Contrast-to-noise ratio (CNR,  $(ROI_{Organ} - ROI_{Muscle}) / noise$ ) [21] and figure of merit (FOM,  $CNR^2 / ED$ ) [22] were calculated.

Two abdominal radiologists were blinded to all technical and personal identifiers to assess the subjective image quality independently. Clinical images were presented at a soft-tissue window and a dedicated liver window (level, 100 HU; width, 200 HU). Subjective image quality, including image noise,

**Table 1.** CT acquisition, contrast injection protocols, and reconstruction parameters.

Parameter	Group A (80 kV)	Group B (100 kV)	Group C (120 kV)
BMI (kg/m <sup>2</sup> )	≤24	24.1-28	≥28.1
CT scanning			
Tube voltage (kV)	80	100	120
Tube current (mA)	Auto	Auto	Auto
FOV (mm)	36	36	36
Gantry rotation time (sec)	0.8	0.8	0.8
Helical pitch	0.984: 1	0.984: 1	0.984: 1
Reconstruction			
Reconstructed section thickness (mm)	5.00	5.00	5.00
Reconstructed section increment (mm)	5.00	5.00	5.00
Reconstruction algorithm	40% ASIR	40% ASIR	40% ASIR
Reconstruction kernel	Soft tissue	Soft tissue	Soft tissue
Contrast Injection			
Contrast medium	Ultravist-300	Ultravist-300	Ultravist-300
Iodine amount (mg I/kg)	352	440	550
Saline (ml)	30	30	30
Injection duration (sec)	25	30	30
Bolus speed (ml/sec)	$\frac{BW \times \frac{352}{300}}{25}$	$\frac{BW \times \frac{440}{300}}{30}$	$\frac{BW \times \frac{550}{300}}{30}$

BMI – body mass index; ASIR – adaptive statistical iterative reconstruction; BW – body weight; ASIR – adaptive statistical iterative reconstruction; FOV – field of view.

vessel sharpness, beam-hardening artifact, reconstruction artifact, and overall image quality, was assessed by 2 observers (Table 2). The degree of conspicuity, representing the ease of discriminating a lesion relative to the background liver, was scored using a 4-point Likert scale (where 1=barely conspicuous, with presence debatable; 2=subtle finding, seemingly a tumor; 3=tumor lesion likely present; and 4=clearly defined and definitely detected tumor) [23].

**Statistical Analysis**

The software packages SPSS (version 12.0, SPSS) and MedCalc (version 19.3, MedCalc Software) were used for data analysis in this study. All the data were expressed as mean±standard deviation unless otherwise indicated. The Kruskal-Wallis 2-way analysis of variance was used if data were not normally distributed. If the result did differ significantly among all the groups, pairwise comparisons were performed by means of the Mann-Whitney U test. Sensitivity, specificity, positive predictive value,

and negative predictive value for each MDCT acquisition protocol were assessed. These assessments were conducted for all cases of hepatocellular carcinoma, and the corresponding 95% confidence intervals (CIs) were calculated based on binomial expression. The interobserver agreement was assessed with the kappa coefficients. The scale was as follows: less than 0.20, poor; 0.21-0.40, fair; 0.41-0.60, moderate; 0.61-0.80, substantial; and 0.81-1.00, almost perfect. Values of P<0.05 were considered statistically significant.

**Results**

**Patient Characteristics and Radiation Dose**

Patient characteristics are provided in Table 3. There were significant differences in contrast medium volume and injection rate among the 3 groups (P<0.001). There were significant differences in CTDI<sub>vol</sub>, DLP, ED, and SSDE among the 3

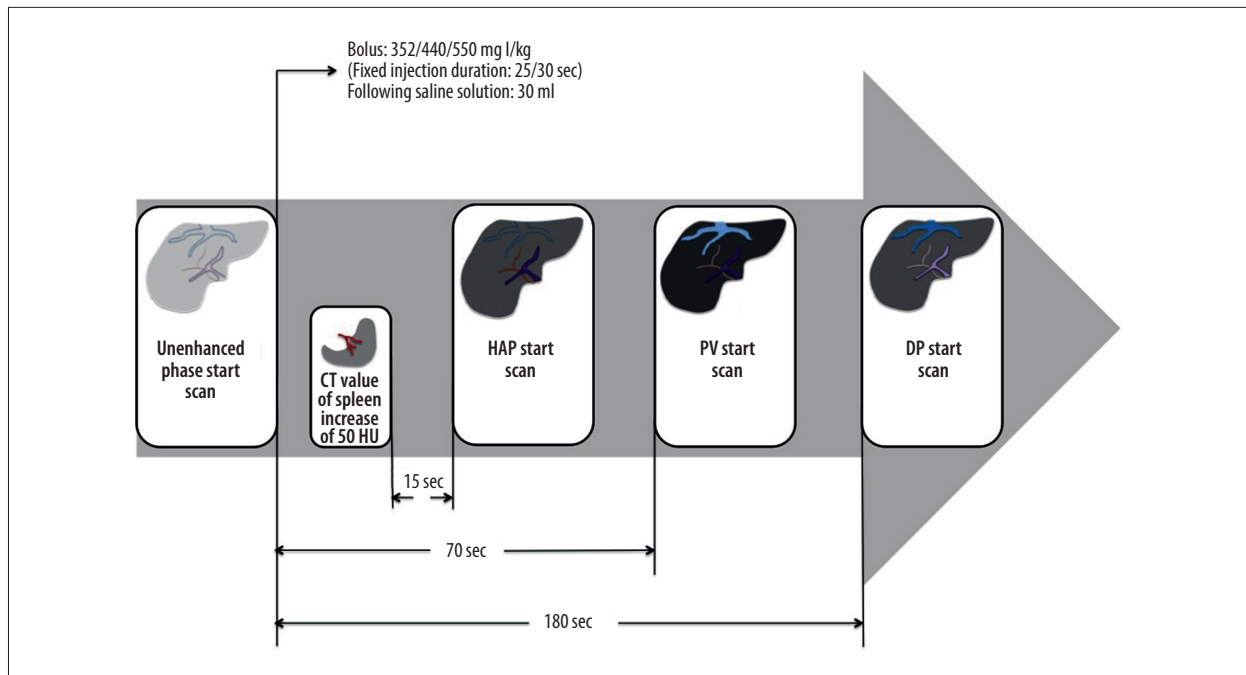


**Figure 2.** Schematic view of splenic-triggering multi-detector row computed tomography (MDCT) scanning protocol. For the multiphase MDCT protocol, patients with different levels of body mass index (BMI) received 352 or 440 or 550 mg I/kg of contrast medium. The injection duration was fixed at 25 s (Group A) or 30 s (Groups B and C), using the same flow rate to inject the contrast medium, followed by 30 ml of saline. The late hepatic arterial phase (HAP) scan was started 15 s after the trigger threshold (set at an increase of 50 HU) was reached in an ROI drawn within the splenic parenchyma at the level of the splenic artery. The portal venous phase (PVP) and delay phase (DP) image scanning started automatically 70 and 180 s after the injection of contrast medium. HU – Hounsfield units; ROI – region of interest.

**Table 2.** Grading scale for subjective image quality analysis of CT examinations.

Qualitative grading scale	Image noise	Vessel sharpness	Beam-hardening artifact	Reconstruction artifact	Overall image quality
1	Unacceptable noise	Blurry border	Many streak artifacts	Many reconstruction artifacts	Unacceptable
2	Above-average noise	Ill-defined border	Moderate streak artifacts	Moderate reconstruction artifacts	Suboptimal
3	Average noise	Defined Border	Minimum streak artifacts	Minimum reconstruction artifacts	Acceptable
4	Less-than-average noise	Clearly defined border	No perceptible streak artifacts	No perceptible reconstruction artifacts	Good
5	Minimum or no noise	Sharply defined border	No perceptible streak artifacts	No perceptible reconstruction artifacts	Superior

The scores of 3-5 for overall image quality were acceptable for diagnosis of liver disease.

**Table 3.** Patient demographic data and radiation dose for multiphasic liver CT studies.

	Group A	Group B	Group C	P value A vs B	P value A vs C	P value B vs C
No. of patients	29	58	39	NA	NA	NA
Patient age (y)	59.2±13.6	61.7±13.6	561.8±10.6	0.420	0.468	0.420
Mean BMI (kg/m <sup>2</sup> )	21.8±1.6	26.00±1.26	29.05±1.0	<.0001	<.0001	<.0001
Mean BW (kg)	58.0±7.3	74.1±7.2	84.2±9.7	<.0001	<.0001	<.0001
Contrast medium volume (ml)	68.1±8.5	108.6±10.6	144.6±9.2	<.0001	<.0001	<.0001
Contrast medium rate (ml/s)	2.7±0.3	3.6±0.4	4.8±0.3	<.0001	<.0001	<.0001
CTDI <sub>vol</sub> (mGy)	4.80±1.78	7.14±0.72	12.23±1.18	<.0001	<.0001	<.0001
DLP (mGy-cm)	129.07±29.65	189.00±33.58	346.67±44.84	<.0001	<.0001	<.0001
Effective dose (mSv)	1.93±0.44	2.84±0.50	5.20±0.67	<.0001	<.0001	<.0001
SSDE (mGy)	7.55±3.11	9.62±1.43	15.08±1.83	<.0001	<.0001	<.0001

Unless otherwise specified, data are means±standard deviations, NA – not applicable; BMI – body mass index; BW – body weight; CTDI<sub>vol</sub> – CT dose index; DLP – dose-length product; SSDE – size-specific dose estimate.

groups ( $P<0.001$ ). Compared with Group C, the radiation doses for Group A and Group B demonstrated a reduction of 61% and 42% in CTDI<sub>vol</sub>, 63% and 45% in ED, and 50% and 36% in SSDE, respectively.

### Timing Adequacy of the Late Arterial Phase

Late arterial phase images obtained for Group A were scored as appropriate in 28 of 29 cases (96.6%) and as early in 1 case. Late arterial phase images obtained for Group B were scored as appropriate in 54 of 58 cases (93.1%), early in 3 cases, and late in 1 case. For Group C, 1 case was considered as early timing for late arterial phase images, and 38 of 39 cases (97.4%) were considered as appropriate. As a result, overall, 95.2% (120 of 126) of the examinations were considered as reflecting adequate timing for late arterial phase.

### Quantitative Image Assessment

The mean CT values for hepatic parenchyma (Group A, 74.97±8.65 HU; Group B, 74.86±10.25 HU; Group C, 76.25±11.29 HU), aorta (Group A, 352.24±43.55 HU; Group B, 314.79±46.01 HU; Group C, 315.05±37.28 HU), portal vein (Group A, 141.59±25.00 HU; Group B, 143.40±28.83 HU; Group C, 144.26±32.39 HU) and pancreas (Group A, 117.24±11.34 HU; Group B, 113.50±13.62 HU; Group C, 116.51±17.69 HU) did not differ significantly among the 3 groups in the late arterial phase ( $P=0.526-0.979$ ) (Figure 3). In 98% of the patients (123/126), the CT value of the hepatic parenchyma in the portal venous phase was enhanced by more than 50 HU as compared with precontrast images. There were 2 cases in Group B

and 1 case in Group C with contrast enhancements of the aorta that were lower than 250 HU during the late arterial phase.

The results of quantitative image analysis are summarized in Table 4. Group A had the highest mean image noise compared with the other 2 groups ( $P=0.002$ ;  $P<0.001$ ). For the liver and portal vein, significantly lower CNRs were found in Group A than in the other 2 groups ( $P=0.001-0.045$ ). Group B had higher CNRs for the liver, blood vessels, and pancreas than Group C ( $P=0.001-0.049$ ). The FOMs of the aorta, portal vein, pancreas, and liver did not differ significantly among Groups A, B, and C ( $P=0.108-0.620$ ).

### Qualitative Image Quality Assessment

The level of interobserver agreement and the qualitative evaluation scores assigned by 2 radiologists are summarized in Table 5. Image noise in Group A was significantly lower than in Group B and Group C ( $P=0.008$ ;  $P<0.001$ ). Group A had a significantly higher score in terms of vessel sharpness than the other 2 groups ( $P=0.037$ ;  $P<0.001$ ). No significant differences in beam-hardening artifact and reconstruction artifact were found among Groups A, B, and C ( $P=0.301$ ;  $P=0.984$ ). In Groups A, B, and C, the difference in overall image quality score was not statistically significant ( $P=0.383$ ). Fair, moderate, and substantial levels of interobserver agreement were found in terms of image noise, vessel sharpness, and beam-hardening artifact among the 3 groups ( $\kappa=0.528-0.838$ ). Moderate and substantial interobserver agreement was seen in terms of overall image quality and reconstructed artifacts among Groups A, B, and C. ( $\kappa=0.639-0.816$ ).

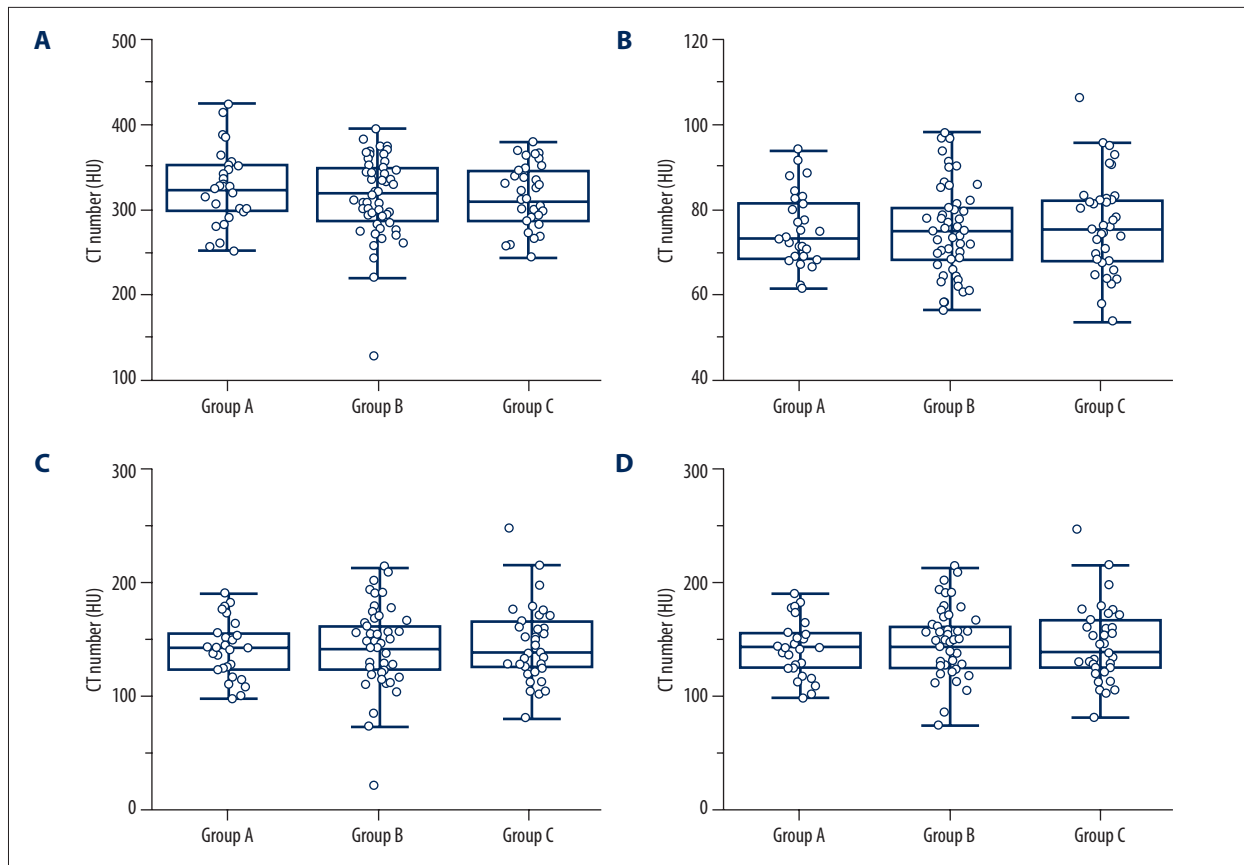


**Figure 3.** Results of quantitative analyses for attenuation values. (A-D) Box-and-whisker plots show attenuation values for hepatic parenchyma (A), aorta (B), main portal vein (C), and pancreas (D), among the 3 CT protocols. The attenuation values for hepatic parenchyma (A), aorta (B), main portal vein (C), and pancreas (D) did not differ significantly among the 3 protocols.

**Table 4.** Quantitative image noise, contrast-to-noise, and figure of merit for the 3 multiphasic liver CT protocols in the late arterial phase.

Characteristic	Group A	Group B	Group C	P value A vs B	P value A vs C	P value B vs C
Image noise	11.61±2.57	9.84±2.13	7.92±1.53	0.002	<.0001	<.0001
Mean CNR						
Liver	1.48±0.98	2.06±1.26	2.67±1.56	0.045	0.001	0.049
Aorta	24.09±6.50	27.57±8.21	33.96±8.16	0.058	<.0001	<.0001
Portal vein	7.55±3.00	9.37±3.99	11.41±4.13	0.019	<.0001	0.005
Pancreas	5.30±1.46	6.20±2.17	8.03±2.93	0.073	<.0001	0.003
<b>P value A vs B vs C</b>						
Mean FOM						
Liver	1.67±1.98	2.13±2.54	1.82±1.78		0.609	
Aorta	327.22±174.54	310.71±211.25	235.77±110.51		0.108	
Portal vein	32.24±32.68	37.57±38.26	28.25 ±21.63		0.620	
Pancreas	15.83±8.54	15.78±12.61	14.02±10.09		0.365	

Unless otherwise specified, data are means±standard deviations. CNR – contrast-to-noise ratio; FOM – figure of merit.

**Table 5.** Qualitative image assessment for the 3 multiphase liver CT protocols in the late arterial phase.

Characteristic	Group A	Group B	Group C	P value	K value for A	K value for B	K value for C
Image noise	3.55±0.51	3.79±0.49	4.10±0.55	<.0001	0.569	0.601	0.748
Vessel sharpness	4.66±0.55	4.31±0.60	4.03±0.71	0.001	0.542	0.569	0.533
Beam-hardening artifact	3.28±0.75	3.48±0.57	3.56±0.50	0.301	0.528	0.838	0.528
Reconstruction artifact	3.76±0.44	3.76±0.43	3.74±0.44	0.984	0.685	0.685	0.816
Overall image quality	4.45±0.69	4.62±0.52	4.67±0.53	0.383	0.647	0.722	0.639

Unless otherwise specified, data are means±standard deviations.

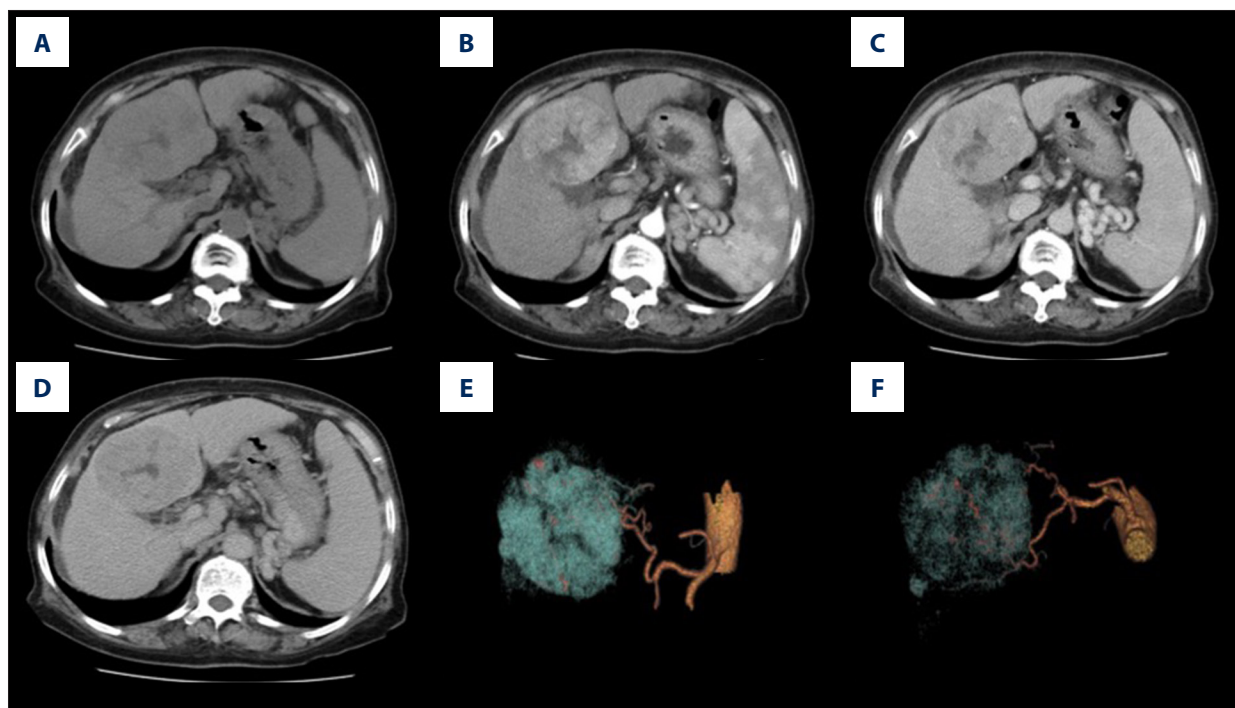


**Figure 4.** Scans from a 75-year-old woman (body mass index, 28.1 kg/m<sup>2</sup>) with hepatitis B cirrhosis. Liver CT was performed at 120 kV (size-specific dose estimate, 16.04 mGy) and contrast medium 550 mg I/kg. (A) Non-enhanced, (B) late arterial, (C) portal venous, and (D) delay phase images; and (E, F) 3D volume-rendering of reconstruction images, with arteries in yellow and tumor in blue. A hypervascular tumor can be seen in the liver, with hypodensity (A), hypervascularity (B), and washout (C, D) relative to the liver parenchyma. Three-dimensional volume-rendering reconstruction images show the relationship between the arteries and the tumor (E, F). The tumor diagnosis of hepatocellular carcinoma was confirmed by pathology.

**Table 6.** Diagnostic accuracy in detection of hepatocellular carcinoma with 3 multiphase liver CT protocols.

Performance Measure	Group A	Group B	Group C
Sensitivity (%)	88.9 (50.7-99.4)	92.9 (79.4-98.1)	92.3 (73.4-98.7)
Specificity (%)	98.7 (91.2-99.9)	97.5 (92.3-99.4)	98.7 (92.1-99.9)
Positive predictive value (%)	88.9 (50.7-99.4)	92.9 (79.4-98.1)	96.0 (77.7-99.8)
Negative predictive value (%)	98.7 (91.2-99.9)	97.5 (92.3-99.4)	97.5 (90.3-99.6)

Data in parentheses represent 95% confidence interval.



Although Group C yielded higher mean scores for HCC conspicuity than did the other 2 groups (Group C vs Group A, 3.62 vs 3.56; Group C vs Group B, 3.62 vs 3.50) (Figure 4), no significant difference was found among the 3 groups ( $P=0.737$ ). Fair and moderate interobserver agreements were found in ratings of the 3 groups ( $\kappa=0.581 \sim 0.753$ ). There was no difference in HCC detection rate among the 3 groups; detection rates were: Group A, mean detection rate=93.8%, 95% CI, 86.3-97.9%; Group B, mean detection rate=95.2%, 95% CI, 90.7-97.9%; and Group C, mean detection rate=95.5%; 95% CI, 89.6-98.6%. Group A had a slightly lower sensitivity and positive predictive value than the other 2 groups (Table 6).

## Discussion

With more concern for radiation risk in recent years, low tube voltage CT has drawn more attention from radiologists [24,25]. Previous studies showed that low tube voltage could reduce the dose of iodine and radiation, without the expense of image quality, in several imaging approaches such as perfusion CT and CTA [13,26]. In the present study, we found that optimization of the CT imaging protocol according to BMI subgroup permitted good image quality for liver CT examination. This is feasible for clinical liver cirrhosis application.

For patients suspected of liver cirrhosis or HCC, the key points of CT image quality are the timing of contrast enhancement, the amplitude of enhancement, and the objective image impression. Also, some studies have pointed out that the desirable enhancement of aorta in the late arterial phase is considered to be 250 HU or more, and that of liver in the portal venous phase is considered to be 50 HU or more [27]. According to these criteria, the protocol for liver CT demands both appropriate enhancement and appropriate timing.

To achieve better enhancement of liver images, some studies have found that the optimal patients' body-weight-tailored dose of iodinated contrast media (CM) ranges from 510-750 mg I/kg for multiphasic MDCT of the liver [28]. Based on our clinical experience, we employed 550 mg I/kg as the optimal body-weight-tailored dose in 120 kV. According to the theoretical algebraic relationship [17], the total amount of iodine load could be reduced to 80% at 100 kV and 64% at 80 kV, compared with that at 120 kV, and still achieve the same contrast enhancement. This result is in fact what we observed in our study (Figure 3). The contrast enhancement of the tissues of the liver cirrhosis patients in our study is in agreement with the conclusions of the previous study, which used both patient weight and contrast concentration to determine the optimized contrast dose [4]. The contrast enhancement of the hepatic parenchyma and blood vessels did not differ significantly among Groups A, B, and C in the late arterial phase. Regarding the influence of the image

noise for the different kVs, the CNRs had significant differences. When combined with the radiation dose, the FOMs returned to a balanced state; showing no differences among the 3 groups.

In order to capture the optimal time window of the late arterial phase, both the scanning protocol and the injection method should be taken into consideration. Previous studies have shown that the injection of CM with fixed duration is appropriate for an individualized liver CT protocol instead of the injection with fixed rate [4,28]. It was shown that the splenic-triggering protocol combined with fixed injection duration was feasible to achieve an enhanced degree of artery imaging [29]. In our study, even though the dose of contrast medium was lower, following the fixed duration injection protocol, we found that 95.2% (120/126) of the cases met the requirements of the LI-RADS standards for the late arterial phase.

A high injection rate is usually recommended to improve the peak enhancement value of aorta and hypervascular focal hepatic lesions [28,29]. In the present study, the concentration of CM was 300 mg I/mL, the fixed injection duration of CM in the 80-kV protocol was 25 s instead of 30 s. The injection rate was 20% higher than that of the 30 s injection duration. The results demonstrated that although the volume and the flow rate in the CM 80-kV protocol were less than those in the 100-kV and 120-kV protocols, we did not observe significant differences in diagnostic performance with respect to HCC among these 3 protocols.

This study had several limitations. First, the comparison of different protocols was based on a small-size sample, and took place in a single center. Second, we employed 550 mg I/kg as the body-weight-tailored dose in the 120 kV condition on account of our clinical experience. We did not compare contrast enhancement between different body-weight-tailored doses of iodinated contrast medium. Third, the diagnostic accuracy for different liver lesions was not investigated. In further studies, more patients should be included to expand the sample size to allow analysis of the detection of liver lesions by LI-RADS standards. At this stage, the individualized CT protocol was determined by technicians at the console according to the patient information. In the future, this categorization and calculation procedure should be automatically integrated into the scanning and injection protocol, for convenience.

## Conclusions

In conclusion, this study demonstrated the feasibility of using an individualized liver contrast-enhanced CT imaging protocol based on BMI, and showed that patients with lower BMI can receive lower contrast dosage and significantly reduced radiation dose.

## Conflict of Interest

None.

## Declaration of Figures Authenticity

All figures submitted have been created by the authors who confirm that the images are original with no duplication and have not been previously published in whole or in part.

## References:

- Islanmi F, Goding Sauer A, Miller KD, et al. Proportion and number of cancer cases and deaths attributable to potentially modifiable risk factors on the United States. *Cancer J Clin.* 2018;68(1):31-54
- Cao MD, Wang H, Shi JF, et al. [Disease burden of liver cancer in China: an updated and integrated analysis on multi-data source evidence] *Zhonghua Liu Xing Bing Xue Za Zhi.* 2020;41(11):1848-58 [in Chinese]
- Chernyak V, Fowler KJ, Kamaya A, et al. Liver imaging reporting and data system (LI-RADS) version 2018: Imaging of hepatocellular carcinoma in at-risk patients. *Radiology.* 2018;289(3):816-30
- Feng ST, Zhu HZ, Peng ZP, et al. An individually optimized protocol of contrast medium injection in enhanced CT scan for liver imaging. *Contrast Media Mol Imaging.* 2017;2017:7350429
- Xu J, He XL, Xiao HW, Xu JG. Comparative study of volume computed tomography dose index and size-specific dose estimate head in computed tomography examination for adult patients based on the mode of automatic tube current modulation. *Med Sci Monit.* 2019;25:71-76
- Kubo T. Vendor free basics of radiation dose reduction techniques for CT. *Eur J Radiol.* 2019;110:14-21
- Higaki T, Nakamura Y, Fukumoto W, et al. Clinical application of radiation dose reduction at abdominal CT. *Eur J Radiol.* 2019;111:68-75
- Bahrami-Motlagh H, Mahboubi-Fooladi Z, Salevatipour B, et al. Comparison of low dose and standard dose abdominal CT scan in body stuffers. *Clin Toxicol.* 2018;56(5):348-54
- Nakaura T, Awai K, Oda S, et al. Low-kilovoltage, high-tube-current MDCT of liver in thin adults: Pilot study evaluating radiation dose, image quality, and display settings. *Am J Roentgenol.* 2011;196(6):1332-38
- Iyama Y, Nakaura T, Yokoyama K, et al. Impact of knowledge-based iterative model reconstruction in abdominal dynamic CT with low tube voltage and low contrast dose. *Am J Roentgenol.* 2016;206(4):687-93
- Kok M, Muhl C, Hendriks BMF, et al. Optimizing contrast media application in coronary CT angiography at lower tube voltage: Evaluation in a circulation phantom and sixty patients. *Eur J Radiol.* 2016;85(6):1068-74
- Pan YY, Zhou SC, Wang YJ, et al. Application of low tube voltage, low-concentration contrast agent using a 320-row CT in coronary CT angiography: Evaluation of image quality, radiation dose and iodine intake. *Curr Med Sci.* 2020;40(1):178-83
- Franzoni CRT, Ippolito D, Riva L, et al. Diagnostic value of iterative reconstruction algorithm in low kV CT angiography (CTA) with low contrast medium volume for transcatheter aortic valve implantation (TAVI) planning: Image quality and radiation dose exposure. *Br J Radiol.* 2018;91(1092):20170802
- Yasunori N, Seitaro O, Takeshi N, et al. Radiation dose reduction at pediatric CT: Use of low tube voltage and iterative reconstruction. *Radiographics.* 2018;38(5):1421-40
- Desai GS, Uppot RN, Yu EW, et al. Impact of iterative reconstruction on image quality and radiation dose in multidetector CT of large body size adults. *Eur Radiol.* 2012;22(8):1631-40
- Lv P, Zhou Z, Liu J, et al. Can virtual monochromatic images from dual-energy CT replace low-kVp images for abdominal contrast-enhanced CT in small- and medium-sized patients? *Eur Radiol.* 2019;29(6):2878-89
- Bae KT. Intravenous contrast medium administration and scan timing at CT: Considerations and approaches. *Radiology.* 2010;256(1):32-61
- Achille M, Daniela BH, Davide B, et al. Adoption of splenic enhancement to time and trigger the late hepatic arterial phase during MDCT of the liver: Proof of concept and clinical feasibility. *Am J Roentgenol.* 2016;207(2):310-20
- Tsalafoutas IA, Hassan KM, Al-Naemi H, et al. Radiation dose monitoring in computed tomography: Status, options and limitations. *Phys Med.* 2020;79:1-15
- Abuhaimed A, Martin CJ. Estimation of size-specific dose estimates (SSDE) for paediatric and adults patients based on a single slice. *Phys Med.* 2020;74:30-39
- Solomon J, Marin D, Choudhury KR, et al. Effect of radiation dose reduction and reconstruction algorithm on image noise, contrast, resolution, and detectability of subtle hypoattenuating liver lesions at multidetector CT: Filtered back projection versus a commercial model-based iterative reconstruction algorithm. *Radiology.* 2017;284(3):777-87
- Borg M, Badr I, Royle GJ. The use of a figure-of-merit (FOM) for optimisation in digital mammography: A literature review. *Radiat Prot Dosimetry.* 2012;151(1):81-88
- Shuman WP, Green DE, Busey JM, et al. Dual-energy liver CT: Effect of monochromatic imaging on lesion detection, conspicuity, and contrast-to-noise ratio of hypervascular lesions on late arterial phase. *Am J Roentgenol.* 2014;203(3):601-6
- Min JC, Sung MK, Tae RA, et al. Comparing feasibility of low-tube-voltage protocol with low-iodine-concentration contrast and high-tube-voltage protocol with high-iodine-concentration contrast in coronary computed tomography angiography. *PLoS One.* 2020;15(7):E0236108
- Matsumoto Y, Masuda T, Sato T, et al. Contrast material injection protocol with the dose determined according to lean body weight at hepatic dynamic computed tomography: Comparison among patients with different body mass indices. *J Comput Assist Tomogr.* 2019;43(5):736-40
- Gawlitza J, Haubenreisser H, Meyer M, et al. Comparison of organ-specific radiation dose levels between 70 kVp perfusion CT and standard tri-phasic liver CT in patients with hepatocellular carcinoma using a Monte-Carlo-Simulation-based analysis platform. *Eur J Radiol.* 2016;3:95-99
- Schindera ST, Winklehner A, Alkadhi H, et al. Effect of automatic tube voltage selection on image quality and radiation dose in abdominal CT angiography of various body sizes: A phantom study. *Clin Radiol.* 2013;68(2):E79-86
- Ichikawa T, Erturk SM, Araki T. Multiphasic contrast-enhanced multidetector-row CT of liver: Contrast-enhancement theory and practical scan protocol with a combination of fixed injection duration and patients' body-weight-tailored dose of contrast material. *Eur J Radiol.* 2006;58(2):165-76
- Eddy K, Costa AF. Assessment of cirrhotic liver enhancement with multiphasic computed tomography using a faster injection rate, late arterial phase, and weight-based contrast dosing. *Can Assoc Radiol J.* 2017;68(4):371-78